Chapter 1
Network of Interdependent Networks: Overview of Theory and Applications

Dror Y. Kenett, Jianxi Gao, Xuqing Huang, Shuai Shao, Irena Vodenska, Sergey V. Buldyrev, Gerald Paul, H. Eugene Stanley and Shlomo Havlin

Abstract Complex networks appear in almost every aspect of science and technology. Previous work in network theory has focused primarily on analyzing single networks that do not interact with other networks, despite the fact that many real-world networks interact with and depend on each other. Very recently an analytical

---

D. Y. Kenett (✉) · J. Gao · X. Huang · S. Shao · G. Paul · H. E. Stanley
Center for Polymer Studies, Department of Physics, Boston university, Boston, MA 02215, USA
e-mail: drorkenett@gmail.com

X. Huang
e-mail: eqing@bu.edu

S. Shao
e-mail: sshao@bu.edu

G. Paul
e-mail: gerryp@bu.edu

H. E. Stanley
e-mail: hes@bu.edu

J. Gao
Department of Automation, Shanghai Jiao Tong, University, 800 Dongchuan Road, Shanghai 200240, People's Republic of China

Center for Complex Network Research and Department of Physics, Northeastern University, Boston, MA02115, USA
e-mail: jianxi.gao@gmail.com

I. Vodenska
Administrative Sciences Department, Metropolitan College, Boston University, Boston, MA 02215, USA
e-mail: vodenska@bu.edu

S. V. Buldyrev
Department of Physics, Yeshiva University, New York, NY10033, USA
e-mail: buldyrev@verizon.net

S. Havlin
Department of Physics, Bar-Ilan University, Ramat Gan, Israel
e-mail: havlins@gmail.com

G. D'Agostino and A. Scala (eds.), *Networks of Networks: The Last Frontier of Complexity*, Understanding Complex Systems, DOI: 10.1007/978-3-319-03518-5_1,

framework for studying the percolation properties of interacting networks has been introduced. Here we review the analytical framework and the results for percolation laws for a network of networks (NON) formed by n interdependent random networks. The percolation properties of a network of networks differ greatly from those of single isolated networks. In particular, although networks with broad degree distributions, e.g., scale-free networks, are robust when analyzed as single networks, they become vulnerable in a NON. Moreover, because the constituent networks of a NON are connected by node dependencies, a NON is subject to cascading failure. When there is strong interdependent coupling between networks, the percolation transition is discontinuous (is a first-order transition), unlike the well-known continuous second-order transition in single isolated networks. We also review some possible real-world applications of NON theory.

1.1 Introduction

The interdisciplinary field of network science has attracted great attention in recent years [1–26]. This has taken place because an enormous amount of data regarding social, economic, engineering, and biological systems has become available over the past two decades as a result of the information and communication revolution brought about by the rapid increase in computing power. The investigation and growing understanding of this extraordinary amount of data will enable us to make the infrastructures we use in everyday life more efficient and more robust. The original model of networks, random graph theory, developed in the 1960s by Erdős and Rényi (ER), is based on the assumption that every pair of nodes is randomly connected with the same probability (leading to a Poisson degree distribution). In parallel, lattice networks in which each node has the same number of links have been used in physics to model physical systems. While graph theory was a well-established tool in the mathematics and computer science literature, it could not adequately describe modern, real-world networks. Indeed, the pioneering observation by Barabási in 1999 [2], that many real networks do not follow the ER model but that organizational principles naturally arise in most systems, led to an overwhelming accumulation of supporting data, new models, and novel computational and analytical results, and led to the emergence of a new science: complex networks.

Significant advances in understanding the structure and function of networks, and mathematical models of networks have been achieved in the past few years. These are now widely used to describe a broad range of complex systems, from techno-social systems to interactions amongst proteins. A large number of new measures and methods have been developed to characterize network properties, including measures of node clustering, network modularity, correlation between degrees of neighboring nodes, measures of node importance, and methods for the identification and extraction of community structures. These measures demonstrated that many real networks, and in particular biological networks, contain network motifs—small specific subnetworks—that occur repeatedly and provide information about functionality [8]. Dynamical processes, such as flow and electrical transport in heterogeneous networks, were shown to be significantly more efficient compared to ER networks [27, 28].

Complex networks are usually non-homogeneous structures that exhibit a power-law form in their degree (number of links per node) distribution. These systems are called scale-free networks. Some examples of real-world scale-free networks include the Internet [3], the WWW [4], social networks representing the relations between individuals, infrastructure networks such as airlines [29, 30], networks in biology, in particular networks of protein-protein interactions [31], gene regulation, and biochemical pathways, and networks in physics, such as polymer networks or the potential energy landscape network. The discovery of scale-free networks has led to a re-evaluation of the basic properties of networks, such as their robustness, which exhibit a character that differs drastically from that of ER networks. For example, while homogeneous ER networks are vulnerable to random failures, heterogeneous scale-free networks are extremely robust [4, 5]. An important property of these infrastructures is their stability, and it is thus important that we understand and quantify their robustness in terms of node and link functionality. Percolation theory was introduced to study network stability and to predict the critical percolation threshold [5]. The robustness of a network is usually (i) characterized by the value of the critical threshold analyzed using percolation theory [32] or (ii) defined as the integrated size of the largest connected cluster during the entire attack process [33]. The percolation approach was also extremely useful in addressing other scenarios, such as efficient attacks or immunization [6, 7, 14, 34, 35], for obtaining optimal path [36] as well as for designing robust networks [33]. Network concepts were also useful in the analysis and understanding of the spread of epidemics [37, 38], and the organizational laws of social interactions, such as friendships [39, 40] or scientific collaborations [41]. Moreira et al. investigated topologically-biased failure in scale-free networks and controlled the robustness or fragility by fine-tuning the topological bias during the failure process [42].

Because current methods deal almost exclusively with individual networks treated as isolated systems, many challenges remain [43]. In most real-world systems an individual network is one component within a much larger complex multi-level network (is part of a network of networks). As technology has advanced, coupling between networks has become increasingly strong. Node failures in one network will cause the failure of dependent nodes in other network, and vice-versa [44]. This recursive process can lead to a cascade of failures throughout the network of networks system. The study of individual particles has enabled physicists to understand the properties of a gas, but in order to understand and describe a liquid or a solid the interactions between the particles also need to be understood. So also in network theory, the study of isolated single networks brings extremely limited results—real-world noninteracting systems are extremely rare in both classical physics and network study. Most real-world network systems continuously interact with other networks, especially since modern technology has accelerated network interdependency.

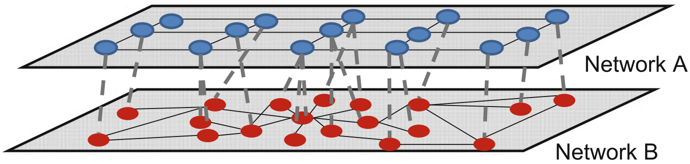

Fig. 1.1 Example of two interdependent networks. Nodes in network B (communications network) are dependent on nodes in network A (power grid) for power; nodes in network A are dependent on network B for control information

To adequately model most real-world systems, understanding the interdependence of networks and the effect of this interdependence on the structural and functional behavior of the coupled system is crucial. Introducing coupling between networks is analogous to the introduction of interactions between particles in statistical physics, which allowed physicists to understand the cooperative behavior of such rich phenomena as phase transitions. Surprisingly, preliminary results on mathematical models [44, 45] show that analyzing complex systems as a network of coupled networks may alter the basic assumptions that network theory has relied on for single networks. Here we will review the main features of the theoretical framework of Network of Networks (NON), and present some real world applications.

1.2 Overview

In order to model interdependent networks, we consider two networks, A and B, in which the functionality of a node in network A is dependent upon the functionality of one or more nodes in network B (see Fig. 1.1), and vice-versa: the functionality of a node in network B is dependent upon the functionality of one or more nodes in network A. The networks can be interconnected in several ways. In the most general case we specify a number of links that arbitrarily connect pairs of nodes across networks A and B. The direction of a link specifies the dependency of the nodes it connects, i.e., link $A_i \rightarrow B_j$ provides a critical resource from node A_i to node B_j. If node A_i stops functioning due to attack or failure, node B_j stops functioning as well but not vice-versa. Analogously, link $B_i \rightarrow A_j$ provides a critical resource from node B_i to node A_j.

To study the robustness of interdependent networks systems, we begin by removing a fraction $1 - p$ of network A nodes and all the A-edges connected to these nodes. As an outcome, all the nodes in network B that are connected to the removed A-nodes by $A \rightarrow B$ links are also removed since they depend on the removed nodes in network A. Their B edges are also removed. Further, the removed B nodes will cause the removal of additional nodes in network A which are connected to the removed B-nodes by $B \rightarrow A$ links. As a result, a cascade of failures that eliminates virtually all nodes in both networks can occur. As nodes and edges are removed, each network breaks up into connected components (clusters). The clusters in network A (connected by A-edges) and the clusters in network B (connected by B-edges) are different since the networks are each connected differently. If one assumes that small clusters (whose size is below certain threshold) become non-functional, this may invoke a recursive process of failures that we now formally describe.

Our insight based on percolation theory is that when the network is fragmented the nodes belonging to the giant component connecting a finite fraction of the network are still functional, but the nodes that are part of the remaining small clusters become non-functional. Thus in interdependent networks only the giant mutually-connected cluster is of interest. Unlike clusters in regular percolation whose size distribution is a power law with a p-dependent cutoff, at the final stage of the cascading failure process just described only a large number of small mutual clusters and one giant mutual cluster are evident. This is the case because the probability that two nodes that are connected by an A-link and their corresponding two nodes are also connected by a B-link scales as $1/N_{\rm B}$, where $N_{\rm B}$ is the number of nodes in network B. So the centrality of the giant mutually-connected cluster emerges naturally and the mutual giant component plays a prominent role in the functioning of interdependent networks. When it exists, the networks preserve their functionality, and when it does not exist, the networks split into fragments so small they cannot function on their own.

We ask three questions: What is the critical $p = p_c$ below which the size of any mutual cluster constitutes an infinitesimal fraction of the network, i.e., no mutual giant component can exist? What is the fraction of nodes $P_\infty(p)$ in the mutual giant component at a given p? How do the cascade failures at each step damage the giant functional component?

Note that the problem of interacting networks is complex and may be strongly affected by variants in the model, in particular by how networks and dependency links are characterized. In the following section we describe several of these model variants.

1.3 Theory of Interdependent Networks

In order to better understand how present-day crucially-important infrastructures interact, Buldyrev et al. [44] recently developed a mathematical framework to study percolation in a system of two coupled interdependent networks subject to cascading failure. Their analytical framework is based on a generating function formalism widely used in studies of single-network percolation and single-network structure [41, 44, 46]. Using the framework to study interdependent networks, we can follow the dynamics of the cascading failures as well as derive analytic solutions for the final steady state. Buldyrev et al. [44] found that interdependent networks were significantly more vulnerable than their noninteracting counterparts. The failure of even a small number of elements within a single network in a system may trigger a catastrophic cascade of events that propagates across the global connectivity. For a

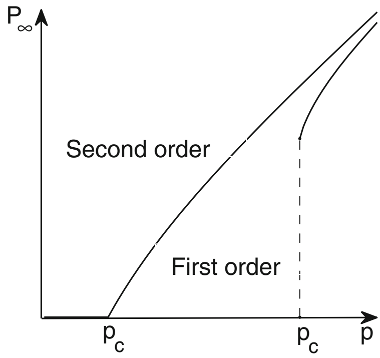

Fig. 1.2 Schematic demonstration of first and second order percolation transitions. In the second order case, the giant component is continuously approaching zero at the percolation threshold $p = p_c$. In the first order case the giant component approaches zero discontinuously. After [47]

fully coupled case in which each node in one network depends on a functioning node in another network and vice versa, Buldyrev et al. [44] found a first-order discontinuous phase transition, which differs significantly from the second-order continuous phase transition found in single isolated networks (Fig. 1.2). This interesting phenomenon is caused by the presence of two types of links: (i) connectivity links within each network and (ii) dependency links between networks. Parshani et al. [45] showed that, when the dependency coupling between the networks is reduced, at a critical coupling strength the percolation transition becomes second-order.

We now present the theoretical methodology used to investigate networks of interdependent networks (see Ref. [47]), and provide examples from different classes of networks.

1.3.1 Generating Functions for a Single Network

We begin by describing the generating function formalism for a single network that is also useful when studying interdependent networks. Here we assume that all N_i nodes in network i are randomly assigned a degree k from a probability distribution $P_i(k)$, and are randomly connected, the only constraint being that the node with degree k has exactly k links [48]. We define the generating function of the degree distribution

$$G_i(x) \equiv \sum_{k=0}^{\infty} P_i(k)x^k, \tag{1.1}$$

where x is an arbitrary complex variable. The average degree of network i is

$$\langle k \rangle_i = \sum_{k=0}^{\infty} kP_i(k) = \left.\frac{\partial G_i}{\partial x}\right|_{x \to 1} = G_i'(1). \tag{1.2}$$

In the limit of infinitely large networks $N_i \to \infty$, the random connection process can be modeled as a branching process in which an outgoing link of any node has a probability $kP_i(k)/\langle k\rangle_i$ of being connected to a node with degree k, which in turn has $k-1$ outgoing links. The generating function of this branching process is defined as

$$H_i(x) \equiv \frac{\sum_{k=0}^{\infty} P_i(k)kx^{k-1}}{\langle k\rangle_i} = \frac{G_i'(x)}{G_i'(1)}. \tag{1.3}$$

The probability f_i that a randomly chosen outgoing link does not lead to an infinitely large giant component satisfies a recursive relation $f_i = H_i(f_i)$. Accordingly, the probability that a randomly chosen node does belong to a giant component is given by $g_i = G_i(f_i)$. Once a fraction $1-p$ of nodes is randomly removed from a network, its generating function remains the same, but must be computed from a new argument $z \equiv px + 1 - p$ [46]. Thus $P_{\infty,i}$, the fraction of nodes that belongs to the giant component, is given by [46],

$$P_{\infty,i} = pg_i(p), \tag{1.4}$$

where

$$g_i(p) = 1 - G_i[pf_i(p) + 1 - p], \tag{1.5}$$

and $f_i(p)$ satisfies

$$f_i(p) = H_i[pf_i(p) + 1 - p]. \tag{1.6}$$

As p decreases, the nontrivial solution $f_i < 1$ of Eq. (1.6) gradually approaches the trivial solution $f_i = 1$. Accordingly, $P_{\infty,i}$—selected as an order parameter of the transition—gradually approaches zero as in the second-order phase transition and becomes zero when two solutions of Eq. (1.6) coincide at $p = p_c$. At this point the straight line corresponding to the right hand side of Eq. (1.6) becomes tangent to the curve corresponding to its left hand side, yielding

$$p_c = 1/H'_i(1). \tag{1.7}$$

For example, for Erdős-Rényi (ER) networks [49–51], characterized by the Poisson degree distribution,

$$G_i(x) = H_i(x) = \exp[\langle k\rangle_i(x-1)], \tag{1.8}$$

$$g_i(p) = 1 - f_i(p), \tag{1.9}$$

$$f_i(p) = \exp\{p\langle k\rangle_i[f_i(p) - 1]\}, \tag{1.10}$$

and

$$p_c = \frac{1}{\langle k\rangle_i}. \tag{1.11}$$

Finally, using Eqs. (1.4), (1.9), and (1.10), one obtains a direct equation for $P_{\infty,i}$

$$P_{\infty,i} = p[1 - \exp(-\langle k \rangle_i P_{\infty,i})]. \quad (1.12)$$

1.3.2 Two Networks with One-to-One Correspondence of Interdependent Nodes

To initiate an investigation of the multitude of problems associated with interacting networks, Buldyrev et al. [44] restricted themselves to the case of two randomly and independently connected networks with the same number of nodes, specified by their degree distributions $P_{\mathrm{A}}(k)$ and $P_{\mathrm{B}}(k)$. They also assumed every node in the two networks to have one B $\rightarrow$ A link and one A $\rightarrow$ B link connecting the same pair of nodes, i.e., the dependencies between networks A and B establish a isomorphism between them that allows us to assume that nodes in A and B coincide (e.g., are at the same corresponding geographic location—if a node in network A fails, the corresponding node in network B also fails, and vice versa). We also assume, however, that the A-edges and B-edges in the two networks are independent.

Unlike the percolation transition in a single network, the mutual percolation transition in this model is a first-order phase transition at which the order parameter (i.e., the fraction of nodes in the mutual giant component) abruptly drops from a finite value at $p_c + \varepsilon$ to zero at $p_c - \varepsilon$. Here ε is a small number that vanishes as the size of network increases $N \rightarrow \infty$. In this range of p, a removal of single critical node may lead to a complete collapse of a seemingly robust network. The size of the largest component drops from $N P_\infty$ to a small value, which rarely exceeds 2.

Note that the value of p_c is significantly larger than in single-network percolation. In two interdependent ER networks, for example, $p_c = 2.4554/\langle k \rangle$, while in a single network, $p_c = 1/\langle k \rangle$. For two interdependent scale-free networks with a power-law degree distribution $P_{\mathrm{A}}(k) \sim k^{-\lambda}$, the mutual percolation threshold is $p_c > 0$, even for $2 < \lambda \leq 3$, when the percolation threshold in a single network is zero.

Note also that, in this new model, networks with a broader degree distribution are less robust against random attack than networks having a narrower degree distribution but the same average degree. This behavior also differs from that found in single networks. To understand this we note that (i) in interdependent networks, nodes are randomly connected—high degree nodes in one network can connect to low degree nodes in other networks, and (ii) at each time step, failing nodes in one network cause their corresponding nodes (and their edges) in the other network to also fail. Thus although hubs in single networks strongly contribute to network robustness, in interdependent networks they are vulnerable to cascading failure. If a network has a fixed average degree, a broader distribution means more nodes with low degree to balance the high degree nodes. Since the low degree nodes are more easily disconnected the advantage of a broad distribution in single networks becomes a disadvantage in interdependent networks.

The following features have been investigated analytically in Ref. [52], a study that assumes that the degrees of the interdependent nodes exactly coincide, but that both networks are randomly and independently connected by their connectivity links. Reference [52] shows that, for two networks with the same degree distribution $P_A(k)$ of connectivity links and random dependency links, studied in Ref. [44], the fraction of nodes in the giant component is

$$P_\infty = p[1 - G_A(z)]^2, \tag{1.13}$$

where $0 \le z \le 1$ is a new variable $z = 1 - p + pf_A$ satisfying equation

$$\frac{[1 - H_A(z)][1 - G_A(z)]}{1 - z} = \frac{1}{p}. \tag{1.14}$$

while in case of coinciding degrees of interdependent nodes Eqs. (1.13) and (1.14) become respectively

$$P_\infty = p[1 - 2G_A(z) + G_A(z^2)] \tag{1.15}$$

and

$$\frac{1 - (1 + z)H_A(z) + zH_A(z^2)}{1 - z} = \frac{1}{p}. \tag{1.16}$$

The left-hand side of Eq. (1.14) always has a single maximum at $0 < z_c < 0$, and the solution abruptly disappear if p becomes less than p_c, the inverse left hand side at z_c. This situation corresponds to the first order transition. In contrast, the left-hand side of Eq. (1.16) has a maximum only if $H'_A(1)$ converges, which corresponds to $\lambda > 3$ when there is a power law tail in the degree distribution. In this case, p_c is the inverse maximum value of the left-hand side of Eq. (1.16), e.g., for ER networks, $p_c = 1.7065/\langle k \rangle$. When $\lambda < 3$, $H'(z)$ diverges for $z \to 1$ and $p_c = 0$, $P_\infty = 0$ as in the case of regular percolation on a single network, for which Eqs. (1.4), (1.5), and (1.6) give

$$P_\infty = p[1 - G_A(z)], \tag{1.17}$$

and

$$\frac{1 - H_A(z)}{1 - z} = \frac{1}{p}. \tag{1.18}$$

Thus for networks with coinciding degrees of the interdependent nodes for $\lambda < 3$, the transition becomes a second-order transition with $p_c = 0$. In the marginal case of $\lambda = 3$, $p_c > 0$, but the transition is second-order.

From Eqs. (1.13)–(1.18) it follows that, if $H'_A(1)$ converges, the networks with coinciding degrees of interdependent nodes are still less robust than single networks, still undergo collapse via a first-order phase transition, but are always more robust than networks with uncorrelated degrees of interdependent nodes. If the average degree is fixed, the robustness of the networks with coinciding degrees of interdependent nodes increases as the degree distribution broadens in the same way as for single networks. Similar observations have been made in numerical studies of interdependent networks with correlated degrees of interdependent nodes [53]. In conclusion, the robustness of interdependent networks increases if the degrees of the interdependent nodes are correlated, i.e., if the hubs are more likely to depend on hubs than on low-degree nodes. For the case of common connectivity links in both networks see Dong et al. [54] and Cellai et al. [55].

1.3.3 Framework of Two Partially Interdependent Networks

A generalization of the percolation theory for two fully interdependent networks was developed by Parshani et al. [45], who studied a more realistic case of a pair of partially-interdependent networks. Here both interacting networks have a certain fraction of completely autonomous nodes whose function does not directly depend on nodes in the other network. They found that when the fraction of autonomous nodes increases above a certain threshold, the collapse of the interdependent networks characterized by a first-order transition observed in Ref. [44] changes, at a critical coupling strength, to a continuous second-order transition as in classical percolation theory [32].

We now describe in more detail the framework developed in [45]. This framework consists of two networks A and B with the number of nodes $N_{\rm A}$ and $N_{\rm B}$, respectively. Within network A, the nodes are randomly connected by A edges with degree distribution $P_{\rm A}(k)$, and the nodes in network B are randomly connected by B edges with degree distribution $P_{\rm B}(k)$. In addition, a fraction $q_{\rm A}$ of network A nodes depends on the nodes in network B and a fraction $q_{\rm B}$ of network B nodes depends on the nodes in network A. We assume that a node from one network depends on no more than one node from the other network, and if A_i depends on B_j, and B_j depends on A_k, then $k = i$. The latter "no-feedback" condition (see Fig. 1.3) disallows configurations that can collapse without taking into account their internal connectivity [56]. Suppose that the initial removal of nodes from network A is a fraction $1 - p$.

We next present the formalism for the cascade process, step by step (see Fig. 1.4). The remaining fraction of network A nodes after an initial removal of nodes is $\psi'_1 \equiv p$. The initial removal of nodes disconnects some nodes from the giant component. The remaining functional part of network A thus contains a fraction $\psi_1 = \psi'_1 g_{\rm A}(\psi'_1)$ of the network nodes, where $g_{\rm A}(\psi'_1)$ is defined by Eqs. (1.5) and (1.6). Since a fraction $q_{\rm B}$ of nodes from network B depends on nodes from network A, the number of nodes in network B that become nonfunctional is $(1 - \psi_1)q_{\rm B} = q_{\rm B}[1 - \psi'_1 g_{\rm A}(\psi'_1)]$. Accordingly, the remaining fraction of network B nodes is $\phi'_1 = 1 - q_{\rm B}[1 - \psi'_1 g_{\rm A}(\psi'_1)]$, and the fraction of nodes in the giant component of network B is $\phi_1 = \phi'_1 g_{\rm B}(\phi'_1)$.

Following this approach we construct the sequence, ψ'_t and ϕ'_t, of the remaining fraction of nodes at each stage of the cascade of failures. The general form is given by

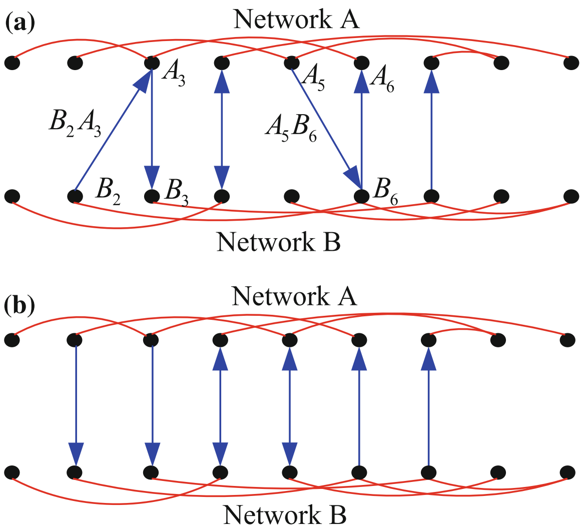

Fig. 1.3 Description of differences between the (**a**) feedback condition and (**b**) no-feedback condition. In the case (**a**), node A_3 depends on node B_2, and node $B_3 \neq B_2$ depends on node A_3, while in case (**b**) this is forbidden. In case (**a**), when $q = 1$ both networks will collapse if one node is removed from one network, which is far from being real. So in our model, we use the no-feedback condition [case (**b**)]. The *blue* links between two networks show the dependency links and the *red* links in each network show the connectivity links which enable each network to function. After [47]

$$\begin{aligned} \psi'_1 &\equiv p, \\ \phi'_1 &= 1 - q_{\rm B}[1 - p g_{\rm A}(\psi'_1)], \\ \psi'_t &= p[1 - q_{\rm A}(1 - g_{\rm B}(\phi'_{t-1}))], \\ \phi'_t &= 1 - q_{\rm B}[1 - p g_{\rm A}(\psi'_{t-1})]. \end{aligned} \tag{1.19}$$

To determine the state of the system at the end of the cascade process we look at ψ'_τ and ϕ'_τ at the limit of $\tau \to \infty$. This limit must satisfy the equations $\psi'_\tau = \psi'_{\tau+1}$ and $\phi'_\tau = \phi'_{\tau+1}$ since eventually the clusters stop fragmenting and the fractions of randomly removed nodes at step τ and $\tau+1$ are equal. Denoting $\psi'_\tau = x$ and $\phi'_\tau = y$, we arrive at the stationary state to a system of two equations with two unknowns,

$$\begin{aligned} x &= p\{1 - q_{\rm A}[1 - g_{\rm B}(y)]\}, \\ y &= 1 - q_{\rm B}[1 - g_{\rm A}(x)p]. \end{aligned} \tag{1.20}$$

The giant components of networks A and B at the end of the cascade of failures are, respectively, $P_{\infty,A} = \psi_\infty = x g_{\rm A}(x)$ and $P_{\infty,B} = \phi_\infty = y g_{\rm B}(y)$. The numerical results were obtained by iterating system (1.19), where $g_{\rm A}(\psi'_t)$ and $g_{\rm B}(\phi'_t)$ are computed using Eqs. (1.9) and (1.10). Figure 1.5 shows excellent agreement between simulations of cascading failures of two partially interdependent networks with $N = 2 \times 10^5$ nodes and the numerical iterations of system (1.19). In the simu-

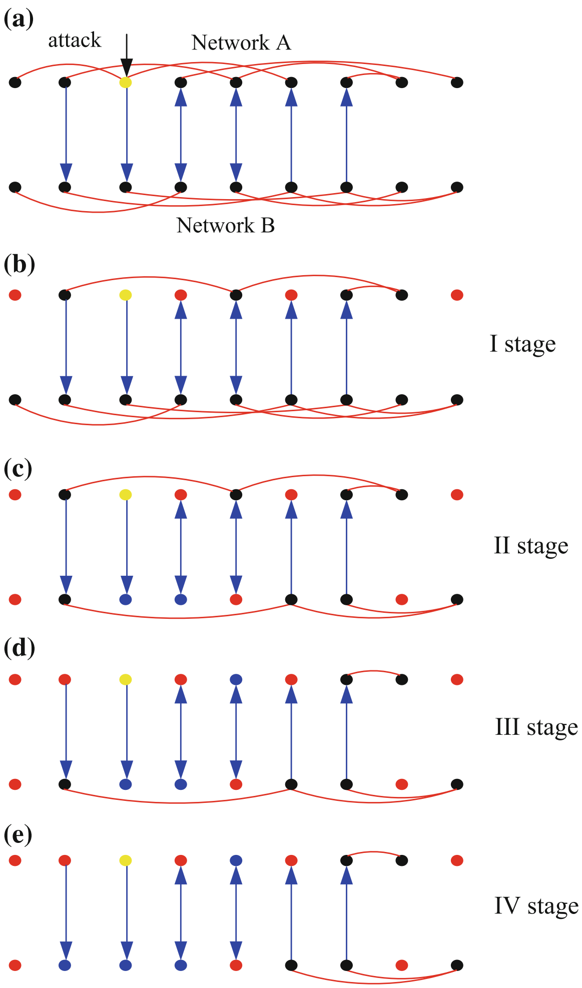

Fig. 1.4 Description of the dynamic process of cascading failures on two partially interdependent networks, which can be generalized to n partially interdependent networks. In this figure, the *black* nodes are the survived nodes, the *yellow* node represents the initially attacked node, the *red* nodes are the nodes removed because they do not belong to the largest cluster, and the *blue* nodes are the nodes removed because they depend on the failed nodes in the other network. In each stage, for one network, we first remove the nodes that depend on the failed nodes in the other network or on the initially attacked nodes. Next we remove the nodes which do not belong to the largest cluster of the network. After [47]

lations, p_c can be determined by the sharp peak in the average number of cascades (iterations), $\langle \tau \rangle$, before the network either stabilizes or collapses [15].

An investigation of Eq. (1.20) can be illustrated graphically by two curves crossing in the (x, y) plane. For sufficiently large q_A and q_B the curves intersect at two points $(0 < x_0, 0 < y_0)$ and $(x_0 < x_1 < 1, y_0 < y_1 < 1)$. Only the second solution (x_1, y_1)

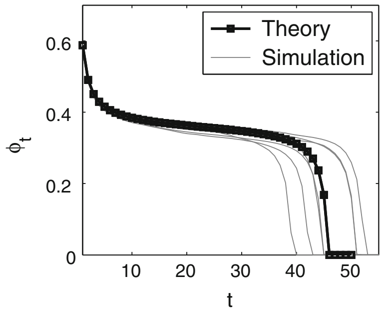

Fig. 1.5 Cascade of failures in two *partially* interdependent ER networks. The giant component ϕ_t for every iteration of the cascading failures is shown for the case of a first order phase transition with the initial parameters $p = 0.8505$, $a = b = 2.5$, $q_A = 0.7$ and $q_B = 0.8$. In the simulations, $N = 2 \times 10^5$ with over 20 realizations. The *gray lines* represent different realizations. The *squares* is the average over all realizations and the *black line* is the theory, Eq. (1.19). After [47]

has any physical meaning. As p decreases, the two solutions become closer to each other, remaining inside the unit square $(0 < x < 1; 0 < y < 1)$, and at a certain threshold $p = p_c$ they coincide: $0 < x_0 = x_1 = x_c < 1$, $0 < y_0 = y_1 = y_c < 1$. For $p < p_c$ the curves no longer intersect and only the trivial solution $g_A(x) = g_B(y) = 0$ remains. For sufficiently large q_A and q_B, $P_{\infty,A}$ and $P_{\infty,B}$ as a function of p show a first order phase transition. As q_B decreases, $P_{\infty,A}$ as a function of p shows a second order phase transition. For the graphical representation of Eq. (1.20) and all possible solutions see Fig. 3 in Ref. [45].

In a recent study [33, 57], it was shown that a pair of interdependent networks can be designed to be more robust by choosing the autonomous nodes to be high degree nodes. This choice mitigates the probability of catastrophic cascading failure.

1.3.4 Framework for a Network of Interdependent Networks

In many real systems there are more than two interdependent networks, and diverse infrastructures—water and food supply networks, communications networks, fuel networks, financial transaction networks, or power station networks—can be coupled together [58]. Understanding the way system robustness is affected by such interdependencies is one of the major challenges when designing resilient infrastructures.

Here we review the generalization of the theory of a pair of interdependent networks [44, 45] to a system of n interacting networks [59, 60], which can be graphically represented (see Fig. 1.6) as a network of networks (NON). We review an exact analytical approach for percolation of an NON system composed of n *fully* or *partially* coupled randomly interdependent networks. The approach is based on analyzing the dynamical process of the cascading failures. The results generalize the

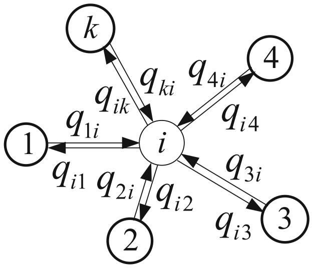

Fig. 1.6 Schematic representation of a network of networks. *Circles* represent interdependent networks, and the *arrows* connect the partially interdependent pairs. For example, a fraction of q_{3i} of nodes in network i depend on the nodes in network 3. The networks which are not connected by the dependency links do not have nodes that directly depend on one another. After [47]

known results for percolation of a single network ($n = 1$) and the $n = 2$ result found in [44, 45], and show that while for $n = 1$ the percolation transition is a second-order transition, for $n > 1$ cascading failures occur and the transition becomes first-order. Our results for n interdependent networks suggest that the classical percolation theory extensively studied in physics and mathematics is a limiting case of $n = 1$ of a general theory of percolation in NON. As we will discuss here, this general theory has many novel features that are not present in classical percolation theory.

In our generalization, each node in the NON is a network itself and each link represents a *fully* or *partially* dependent pair of networks. We assume that each network i ($i = 1, 2, ..., n$) of the NON consists of N_i nodes linked together by connectivity links. Two networks i and j form a partially dependent pair if a certain fraction $q_{ji} > 0$ of nodes of network i directly depends on nodes of network j, i.e., they cannot function if the nodes in network j on which they depend do not function. Dependent pairs are connected by unidirectional dependency links pointing from network j to network i. This convention indicates that nodes in network i get a crucial commodity from nodes in network j, e.g., electric power if network j is a power grid.

We assume that after an attack or failure only a fraction of nodes p_i in each network i will remain. We also assume that only nodes that belong to a giant connected component of each network i will remain functional. This assumption helps explain the cascade of failures: nodes in network i that do not belong to its giant component fail, causing failures of nodes in other networks that depend on the failing nodes of network i. The failure of these nodes causes the direct failure of dependency nodes in other networks, failures of isolated nodes in them, and further failure of nodes in network i and so on. Our goal is to find the fraction of nodes $P_{\infty,i}$ of each network that remain functional at the end of the cascade of failures as a function of all fractions p_i and all fractions q_{ij}. All networks in the NON are randomly connected networks characterized by a degree distribution of links $P_i(k)$, where k is a degree of a node in network i. We further assume that each node a in network i may depend with probability q_{ji} on only one node b in network j with no feed-back condition.

To study different models of cascading failures, we vary the survival time of the dependent nodes after the failure of the nodes in other networks on which they depend, and the survival time of the disconnected nodes. We conclude that the final state of the networks does not depend on these details but can be described by a system of equations somewhat analogous to the Kirchhoff equations for a resistor network. This system of equations has n unknowns x_i. These represent the fraction of nodes that survive in network i after the nodes that fail in the initial attack are removed and the nodes depending on the failed nodes in other networks at the end of cascading failure are also removed, but without taking into account any further node failure due to the internal connectivity of the network. The final giant component of each network is $P_{\infty,i} = x_i g_i(x_i)$, where $g_i(x_i)$ is the fraction of the remaining nodes of network i that belongs to its giant component given by Eq. (1.5).

The unknowns x_i satisfy the system of n equations, [53]

$$x_i = p_i \prod_{j=1}^{K} [q_{ji} y_{ji} g_j(x_j) - q_{ji} + 1], \tag{1.21}$$

where the product is taken over the K networks interlinked with network i by partial dependency links (see Fig. 1.6) and

$$y_{ij} = \frac{x_i}{p_j q_{ji} y_{ji} g_j(x_j) - q_{ji} + 1}, \tag{1.22}$$

is the fraction of nodes in network j that survives after the damage from all the networks connected to network j except network i is taken into account. The damage from network i must be excluded due to the no-feedback condition. In the absence of the no-feedback condition, Eq. (1.21) becomes much simpler since $y_{ji} = x_j$. Equation (1.21) is valid for any case of interdependent NON, while Eq. (1.22) represents the no-feedback condition.

A more the most general case of interdependency links was studied by Shao et al. [56]. They assumed that a node in network i is connected by s supply links to s nodes in network j from which it gets a crucial commodity. If $s = \infty$, the node does not depend on nodes in network j and can function without receiving any supply from them. The generating function of the degree distribution $P^{ij}(s)$ of the supply links $G^{ji}(x) = \sum_{i=0}^{\infty} P^{ji}(s) x^s$ does not include the term $P^{ji}(\infty) = 1 - q_{ji}$, and hence $G_{ji}(1) = q_{ji} \leq 1$. It is also assumed that nodes with $s < \infty$ can function only if they are connected to at least one functional node in network j. In this case, Eq. (1.21) must be changed to

$$x_i = p_i \prod_{j=1}^{K} \{1 - G^{ji}[1 - x_j g_j(x_j)\}. \tag{1.23}$$

When all dependent nodes have exactly one supply link, $G_{ij}(x) = x q_{ij}$ and Eq. (1.23) becomes

$$x_i = p_i \prod_{j=1}^{K} [1 - q_{ji} + q_{ji} x_j g_j(x_j)], \tag{1.24}$$

analogous to Eq. (1.21) without the no-feedback condition.

1.3.5 Examples of Classes of Network of Networks

Finally, we present four examples that can be explicitly solved analytically: (i) a tree-like ER NON *fully* dependent, (ii) a tree-like random regular (RR) NON *fully* dependent, (iii) a loop-like ER NON *partially* dependent, and (iv) an RR network of *partially* dependent ER networks. All cases represent different generalizations of percolation theory for a single network.

1.3.5.1 Tree-Like NON of ER Networks

We solve explicitly the case of a tree-like NON (see Fig. 1.7) formed by n ER [49–51] networks with average degrees $k_1, k_2, ...k_i, ..., k_n$, $p_1 = p$, $p_i = 1$ for $i \neq 1$ and $q_{ij} = 1$ (fully interdependent). Using Eqs. (1.21) and (1.22) for x_i and taking into account Eqs. (1.8), (1.9) and (1.10), we find that

$$f_i = \exp\left[-pk_i \prod_{j=1}^{n} (1 - f_j)\right], i = 1, 2, ..., n. \tag{1.25}$$

These equations can be solved analytically [59]. They have only a trivial solution ($f_i = 1$) if $p < p_c$, where p_c is the mutual percolation threshold. When the n networks have the same average degree k, $k_i = k$ ($i = 1, 2, ..., n$), we obtain from Eq. (1.25) that $f_c \equiv f_i(p_c)$ satisfies

$$f_c = \exp\left[\frac{f_c - 1}{nf_c}\right]. \tag{1.26}$$

where the solution can be expressed in terms of the Lambert function $W_-(x)$, $f_c = -[nW_-(-\frac{1}{n}e^{-\frac{1}{n}})]^{-1}$, where $W_-(x)$ is the most negative of the two real roots of the Lambert equation $e^{[W(x)]W(x)=x}$ for $x < 0$.

Once f_c is known, we can obtain p_c and the giant component at p_c $P_{\infty,n} \equiv P_\infty$

$$\begin{aligned} p_c &= [nkf_c(1 - f_c)^{(n-1)}]^{-1}, \\ P_\infty(p_c) &= \frac{1-f_c}{nkf_c}. \end{aligned} \tag{1.27}$$

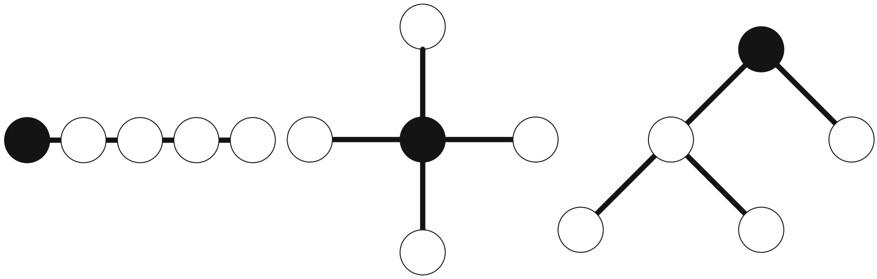

Fig. 1.7 Three types of loopless networks of networks composed of five coupled networks. All have same percolation threshold and same giant component. The *dark* node is the origin network on which failures initially occur. After [47]

Equation (1.27) generalizes known results for $n = 1, 2$. For $n = 1$, we obtain the known result $p_c = 1/k$, Eq. (1.11), of an ER network [49–51] and $P_\infty(p_c) = 0$, which corresponds to a continuous second-order phase transition. Substituting $n = 2$ in Eqs. (1.26) and (1.27) yields the exact results of [44].

From Eqs. (1.21)–(1.22) we obtain an exact expression for the order parameter $P_\infty(p_c)$, the size of the mutual giant component for all p, k, and n values,

$$P_\infty = p[1 - \exp(-kP_\infty)]^n. \tag{1.28}$$

Solutions of Eq. (1.28) are shown in Fig. 1.8a for several values of n. Results are in excellent agreement with simulations. The special case $n = 1$ is the known ER second-order percolation law, Eq. (1.12), for a single network [49–51]. In contrast, for any $n > 1$ the solution of (1.28) yields a first-order percolation transition, i.e., a discontinuity of P_∞ at p_c.

To analyze p_c as a function of n for different k values, we find f_c from Eq. (1.26), substitute it into Eq. (1.27), and obtain p_c. Figure 1.8 shows that the NON becomes more vulnerable with increasing n or decreasing k (p_c increases when n increases or k decreases). Furthermore, when n is fixed and k is smaller than a critical number $k_{\min}(n)$, $p_c \geq 1$, which means that when $k < k_{\min}(n)$ the NON will collapse even if a single node fails. The minimum average degree $k_{\min}$ as a function of the number of networks is

$$k_{\min}(n) = [nf_c(1 - f_c)^{(n-1)}]^{-1}. \tag{1.29}$$

Equations (1.25)–(1.29) are valid for all tree-like structures such as those shown in Fig.1.7. Note that Eq. (1.29) together with Eq. (1.26) yield the value of $k_{\min}(1) = 1$, reproducing the known ER result, that $\langle k \rangle = 1$ is the minimum average degree needed to have a giant component. For $n = 2$, Eq. (1.29) also yields results obtained in [44], i.e., $k_{\min} = 2.4554$.

1.3.5.2 Tree-Like NON of RR Networks

We review the case of a tree-like network of interdependent RR networks [59, 61] in which the degree of each network is assumed to be the same k (Fig. 1.7). By introducing a new variable $r = f^{\frac{1}{k-1}}$ into Eqs. (1.21) and (1.22) and the generating function of RR network [59], the n equations reduce to a single equation

$$r = (r^{k-1} - 1)p(1 - r^k)^{n-1} + 1, \tag{1.30}$$

which can be solved graphically for any p. The critical case corresponds to the tangential condition leading to critical threshold p_c and P_∞

$$p_c = \frac{r - 1}{(r^{k-1} - 1)(1 - r^k)^{n-1}}, \tag{1.31}$$

$$P_\infty = p\left(1 - \left\{p^{\frac{1}{n}} P_\infty^{\frac{n-1}{n}}\left[\left(1 - \left(\frac{P_\infty}{p}\right)^{\frac{1}{n}}\right)^{\frac{k-1}{k}} - 1\right] + 1\right\}^k\right)^n. \tag{1.32}$$

Comparing this with the results of a tree-like ER NON, we find that the robustness of n coupled RR networks of degree k is significantly higher than the n interdependent ER networks of average degree k. Although for an ER NON there exists a critical minimum average degree $k = k_{\min}$ that increases with n below which the system collapses, there is no such analogous $k_{\min}$ for a RR NON system. For any $k > 2$, the RR NON is stable, i.e., $p_c < 1$. In general, this is the case for any network with any degree distribution such that $P_i(0) = P_i(1) = 0$, i.e., for a network without disconnected and singly-connected nodes [61].

1.3.5.3 Loop-Like NON of ER Networks

In the case of a loop-like NON (for dependencies in one direction) of n ER networks, all the links are unidirectional and the no-feedback condition is irrelevant. If the initial attack on each network is the same $1 - p$, $q_{i-1i} = q_{n1} = q$, and $k_i = k$, using Eqs. (1.21) and (1.22) we find that P_∞ satisfies

$$P_\infty = p(1 - e^{-kP_\infty})(qP_\infty - q + 1). \tag{1.33}$$

Note that when $q = 1$ Eq. (1.33) has only a trivial solution $P_\infty = 0$, but when $q = 0$ it yields the known giant component of a single network, Eq. (1.12), as expected. We present in Fig. 1.8b numerical solutions of Eq. (1.33) for two values of q. Note that when $q = 1$ and the structure is tree-like, Eqs. (1.28) and (1.32) depend on n, but for loop-like NON structures, Eq. (1.33) is independent of n.

1.3.5.4 RR Network of ER Networks

Now we review results [47] for a NON in which each ER network is dependent on exactly m other ER networks. This system represents the case of RR network of ER networks. We assume that the initial attack on each network is $1 - p$, and each partially dependent pair has the same q in both directions with no-feedback condition. The n equations of Eq. (1.21) are exactly the same due to symmetries, and hence p_c and P_∞ can be solved analytically,

$$p_c^{II} = \frac{1}{k(1-q)^m}, \tag{1.34}$$

$$P_\infty = \frac{p}{2^m}(1 - e^{-kP_\infty})[1 - q + \sqrt{(1-q)^2 + 4qP_\infty}]^m. \tag{1.35}$$

where p_c^{II} denotes the critical threshold for the second order phase transition.

Again, as in the case of the loop-like structure, it is surprising that both the critical threshold and the giant component do not depend on the number of networks n, in contrast to tree-like NON, but only on the coupling q and on both degrees k and m. Numerical solutions of Eq. (1.35) are shown in Fig. 1.8. In the special case of $m = 0$, Eqs. (1.34) and (1.35) coincide with the known results for a single ER network, Eqs. (1.11) and (1.12) separately. It can be shown that when $q < q_c$ we have "weak coupling" represented by a second-order phase transition and when $q_c < q < q_{\max}$ we have "strong coupling" and a first-order phase transition. When $q > q_{\max}$ the system become unstable due to the "very strong coupling" between the networks. In the last case, removal of a single node in one network may lead to the collapse of the NON.

1.3.6 Resilience of Networks to Targeted Attacks

In real-world scenarios, initial system failures seldom occur randomly and can be the result of targeted attacks on central nodes. Such attacks can also occur in less central nodes in an effort to circumvent central node defences, e.g., heavily-connected Internet hubs tend have more effective firewalls. Targeted attacks on high degree nodes [4, 6, 7, 13, 42] or high betweenness nodes [62] in *single* networks dramatically affect their robustness. To study the targeted attack problem on interdependent networks [13, 63–65] we assign a value $W_\alpha(k_i)$ to each node, which represents the probability that a node i with k_i degree will be initially attacked and become inactive, i.e.,

$$W_\alpha(k_i) = \frac{k_i^\alpha}{\sum_{i=1}^N k_i^\alpha}, -\infty < \alpha < +\infty. \tag{1.36}$$

When $\alpha > 0$, higher-degree nodes are more vulnerable to intentional attack. When $\alpha < 0$, higher-degree nodes are less vulnerable and have a lower probability of failure. The case $\alpha = 0$, $W_0 = \frac{1}{N}$, represents the random removal of nodes [44].

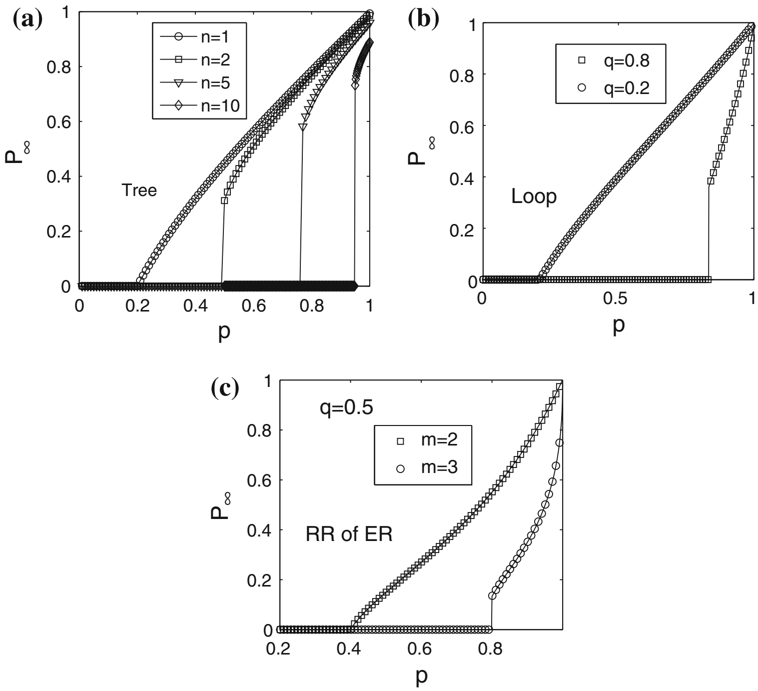

Fig. 1.8 The fraction of nodes in the giant component P_∞ as a function of p for three different examples discussed in Sects. 1.3.5.2–1.3.5.4. (**a**) For a tree-like *fully* ($q = 1$) interdependent NON is shown P_∞ as a function of p for $k = 5$ and several values of n. The results obtained using Eq. (1.28). Note that increasing n from $n = 2$ yields a first order transition. (**b**) For a loop-like NON, P_∞ as a function of p for $k = 6$ and two values of q. The results obtained using Eq. (1.33). Note that increasing q yields a first order transition. (**c**) For an RR network of ER networks, P_∞ as a function of p, for two different values of m when $q = 0.5$. The results are obtained using Eq. (1.35) , and the number of networks, n, can be any number with the condition that any network in the NON connects exactly to m other networks. Note that changing m from 2 to $m > 2$ changes the transition from second order to first order (for $q = 0.5$). Simulation results are in excellent agreement with theory. After [47]

In the interdependent networks model with networks A and B described in Ref. [44], a fraction $1 - p$ of the nodes from one network are removed with a probability $W_\alpha(k_i)$ [Eq. (1.36)]. The cascading failures are then the same as those described in Ref. [44]. To analytically solve the targeted attack problem we must find an equivalent network A', such that the *targeted* attack problem on interdependent networks A and B can be solved as a *random* attack problem on interdependent networks A' and B. We begin by finding the new degree distribution of network A after using Eq. (1.36) to remove a $1 - p$ fraction of nodes but before the links of the remaining nodes that connect to the removed nodes are removed. If $A_p(k)$ is the number of nodes with degree k and $P_p(k)$ the new degree distribution of the remaining fraction p of nodes in network A, then

$$P_p(k) = \frac{A_p(k)}{pN}. \tag{1.37}$$

When another node is removed, $A_p(k)$ changes as

$$A_{(p-1/N)}(k) = A_p(k) - \frac{P_p(k)k^\alpha}{\langle k(p)^\alpha \rangle}, \tag{1.38}$$

where $\langle k(p)^\alpha \rangle \equiv \sum P_p(k)k^\alpha$. In the limit of $N \to \infty$, Eq. (1.38) can be presented in terms of a derivative of $A_p(k)$ with respect to p,

$$\frac{dA_p(k)}{dp} = N\frac{P_p(k)k^\alpha}{\langle k(p)^\alpha \rangle}. \tag{1.39}$$

Differentiating Eq. (1.37) with respect to p and using Eq. (1.39), we obtain

$$-p\frac{dP_p(k)}{dp} = P_p(k) - \frac{P_p(k)k^\alpha}{\langle k(p)^\alpha \rangle}, \tag{1.40}$$

which is exact for $N \to \infty$. In order to solve Eq. (1.40), we define a function $G_\alpha(x) \equiv \sum_k P(k)x^{k^\alpha}$, and substitute $f \equiv G_\alpha^{-1}(p)$. We find by direct differentiation that [46]

$$P_p(k) = P(k)\frac{f^{k^\alpha}}{G_\alpha(f)} = \frac{1}{p}P(k)f^{k^\alpha}, \tag{1.41}$$

$$\langle k(p)^\alpha \rangle = \frac{fG'_\alpha(f)}{G_\alpha(f)}, \tag{1.42}$$

satisfy the Eq. (1.40). With this degree distribution, the generating function of the nodes left in network A before removing the links to the removed nodes is

$$G_{Ab}(x) \equiv \sum_k P_p(k)x^k = \frac{1}{p}\sum_k P(k)f^{k^\alpha}x^k. \tag{1.43}$$

Because network A is randomly connected, the probability of a link emanating from a remaining node is equal to the ratio of the number of links emanating from the remaining nodes to the total number of links emanating from all the nodes of the original network,

$$\tilde{p} \equiv \frac{pN\langle k(p)\rangle}{N\langle k\rangle} = \frac{\sum_k P(k)kf^{k^\alpha}}{\sum_k P(k)k}, \tag{1.44}$$

where $\langle k\rangle$ is the average degree of the original network A, and $\langle k(p)\rangle$ is the average degree of remaining nodes before the links that are disconnected are removed. Removing the links that connect to the deleted nodes of a randomly connected network is equivalent to randomly removing a $(1 - \tilde{p})$ fraction of links of the remaining

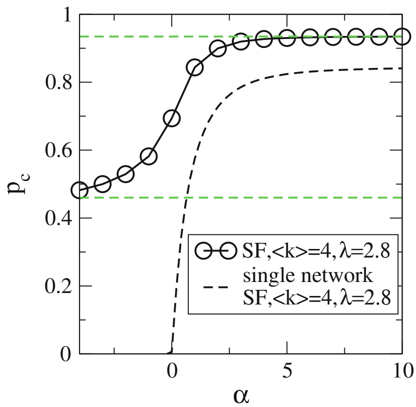

Fig. 1.9 Dependence of p_c on α for SF single and interdependent networks with average degree $\langle k \rangle = 4$ for targeted attacks described in Sect. 3.5. The *lower* cut-off of the degree is $m = 2$. The horizontal lines represent the *upper* and *lower* limits of p_c. The *black dashed line* represents p_c for single SF network. After [63]

nodes. It is known [46] that the generating function of the remaining nodes after random removal of $(1 - \tilde{p})$ fraction of links is equal to the original distribution of the network with a new argument $z = 1 - \tilde{p} + x\tilde{p}$. Thus the generating function of the new degree distribution of the nodes left in network A after their links to the removed nodes are also removed is

$$G_{Ac}(x) \equiv G_{Ab}(1 - \tilde{p} + \tilde{p}x). \tag{1.45}$$

The only difference in the cascading process under *targeted* attack from the case under *random* attack is in the first stage when network A is attacked. If we find a network A' with generating function $\tilde{G}_{A0}(x)$ such that after a random attack with a $(1 - p)$ fraction of nodes removed the generating function of nodes left in A' is the same as $G_{Ac}(x)$, then the targeted attack problem on interdependent networks A and B can be solved as a random attack problem on interdependent networks A' and B. We find $\tilde{G}_{A0}(x)$ by solving the equation $\tilde{G}_{A0}(1 - p + px) = G_{Ac}(x)$ and from, Eq. (1.45),

$$\tilde{G}_{A0}(x) = G_{Ab}(1 + \frac{\tilde{p}}{p}(x - 1)). \tag{1.46}$$

This formalism allows us to map the problem of cascading node failure in interdependent networks caused by an initial *targeted* attack to the problem of *random* attack. We note that the evolution of equations only depends on the generating function of network A, and not on any information concerning how the two networks interact with each other. Thus this approach can be applied to the study of other general interdependent network models.

Finally we analyze the specific class of scale-free (SF) networks. Figure 1.9 shows the critical thresholds p_c of SF networks. Note that p_c in interdependent SF networks is nonzero for the entire range of α because failure of the least-connected nodes in one network may lead to failure of well-connected nodes in a second network, making interdependent networks significantly more difficult to protect than a single network. A significant role in the vulnerability to random attacks is also played by network assortativity [66].

1.3.7 Interdependent Clustered Networks

Clustering quantifies the propensity of two neighbors of the same vertex to also be neighbors of each other, forming triangle-shaped configurations in the network [1, 10, 67]. Unlike random networks in which there is little or no clustering, real-world networks exhibit significant clustering. Recent studies have shown that, for single isolated networks, both bond percolation and site percolation have percolation and epidemic thresholds that are higher than those in unclustered networks [68–73]. Here we review a mathematical framework for understanding how the robustness of interdependent networks is affected by clustering within the network components. We extend the percolation method developed by Newman [68] for single clustered networks to coupled clustered networks. Huang et al. [65] found that interdependent networks that exhibit significant clustering are more vulnerable to random node failure than networks with low significant clustering. They studied two networks, A and B, each having the same number of nodes N. The N nodes in A and B have bidirectional dependency links to each other, establishing a one-to-one correspondence. Thus the functioning of a node in network A depends on the functioning of the corresponding node in network B and vice versa. Each network is defined by a joint degree distribution P_{st} (generating function $G_0(x, y) = \sum_{s,t=0}^{\infty} P_{st} x^s y^t$) that specifies the fraction of nodes connected to s single edges and t triangles [68]. The conventional degree of each node is thus $k = s + 2t$. The clustering coefficient c is

$$c = \frac{\sum_{st} t P_{st}}{\sum_k k(k-1)P(k)/2}. \tag{1.47}$$

1.3.7.1 Percolation on Interdependent Clustered Networks

To study how clustering within interdependent networks affects a system's robustness, we apply the interdependent networks framework [44]. In interdependent networks A and B, a fraction $(1 - p)$ of nodes is first removed from network A. Then the size of the giant components of networks A and B in each cascading failure step is defined to be p_1, p_2, ..., p_n, which are calculated iteratively

$$\begin{aligned} p_n &= \mu_{n-1} g_A(\mu_{n-1}), \text{ n is odd}, \\ p_n &= \mu_n g_B(\mu_n), \text{ n is even}, \end{aligned} \tag{1.48}$$

where $\mu_0 = p$ and μ_n are intermediate variables that satisfy

$$\begin{aligned} \mu_n &= p g_{\mathrm{A}}(\mu_{n-1}), \text{ n is odd,} \\ \mu_n &= p g_{\mathrm{B}}(\mu_{n-1}), \text{ n is even.} \end{aligned} \tag{1.49}$$

As interdependent networks A and B form a stable mutually-connected giant component, $n \to \infty$ and $\mu_n = \mu_{n-2}$, the fraction of nodes left in the giant component is p_∞. This system satisfies

$$\begin{aligned} x &= p g_{\mathrm{A}}(y), \\ y &= p g_{\mathrm{B}}(x), \end{aligned} \tag{1.50}$$

where the two unknown variables x and y can be used to calculate $p_\infty = x g_{\mathrm{B}}(x) = y g_{\mathrm{A}}(y)$. Eliminating y from these equations, we obtain a single equation

$$x = p g_{\mathrm{A}}[p g_{\mathrm{B}}(x)]. \tag{1.51}$$

The critical case ($p = p_c$) emerges when both sides of this equation have equal derivatives,

$$1 = p^2 \frac{dg_{\mathrm{A}}}{dx}[p g_{\mathrm{B}}(x)] \frac{dg_{\mathrm{B}}}{dx}(x)|_{x=x_c, p=p_c}, \tag{1.52}$$

which, together with Eq. (1.51), yields the solution for p_c and the critical size of the giant mutually-connected component, $p_\infty(p_c) = x_c g_{\mathrm{B}}(x_c)$.

Consider for example the case in which networks A and B have Poisson degree distributions P^A_{st} and P^B_{st} for both s and t:

$$\begin{aligned} P^A_{st} &= e^{-\mu_{\mathrm{A}} - \nu_{\mathrm{A}}} \frac{\mu^s_{\mathrm{A}} \nu^t_{\mathrm{A}}}{s!t!}, \\ P^B_{st} &= e^{-\mu_{\mathrm{B}} - \nu_{\mathrm{B}}} \frac{\mu^s_{\mathrm{B}} \nu^t_{\mathrm{B}}}{s!t!}. \end{aligned} \tag{1.53}$$

Using techniques in Ref. [68] it is possible to show that in this case $x = p(1 - u_{\mathrm{A}})$, $y = p(1 - u_{\mathrm{B}})$, where

$$\begin{aligned} u_{\mathrm{A}} = v_{\mathrm{A}} &= e^{[\mu_{\mathrm{A}} y + 2y(1-y)\mu_{\mathrm{A}}](u_{\mathrm{A}}-1) + \nu_{\mathrm{A}} p^2 (v^2_{\mathrm{A}} - 1)}, \\ u_{\mathrm{B}} = v_{\mathrm{B}} &= e^{[\mu_{\mathrm{B}} x + 2x(1-x)\mu_{\mathrm{B}}](u_{\mathrm{B}}-1) + \nu_{\mathrm{B}} p^2 (v^2_{\mathrm{B}} - 1)}. \end{aligned} \tag{1.54}$$

If the two networks have the same clustering, $\mu \equiv \mu_{\mathrm{A}} = \mu_{\mathrm{B}}$ and $\nu \equiv \nu_{\mathrm{A}} = \nu_{\mathrm{B}}$, p_∞ is then

$$p_\infty = p(1 - e^{\nu p^2_\infty - (\mu + 2\nu) p_\infty})^2. \tag{1.55}$$

Here μ and ν are the average number of single links and triangles per node respectively.

The giant component, p_∞, for interdependent clustered networks can thus be obtained by solving Eq. (1.55). Note that when $\nu = 0$ we obtain from Eq. (1.55) the

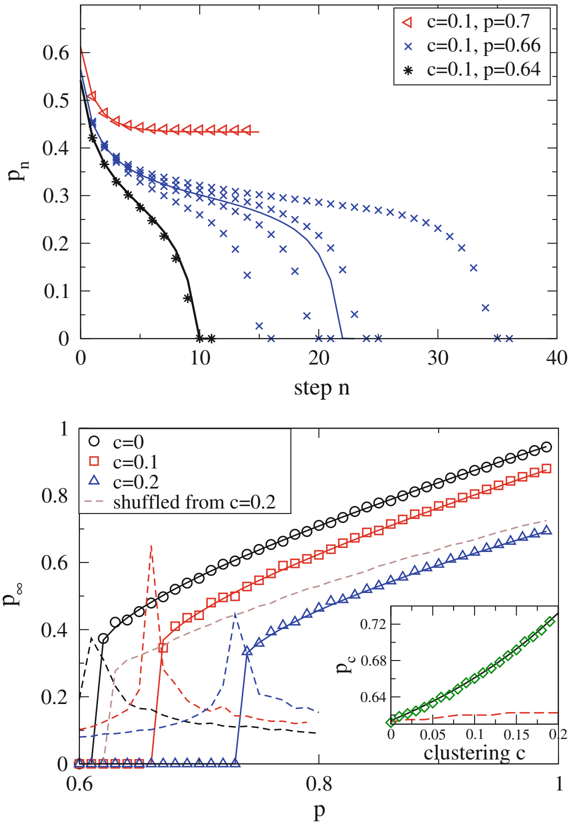

Fig. 1.10 Behavior of interdependent networks with different clustering coefficients. **a** Size of mutually connected giant component as a function of cascading failure steps n. Results are for $c = 0.1$, $p = 0.64$ (*below* p_c), $p = 0.66$ (at p_c) and $p = 0.7$ (*above* p_c). Lines represent theory (Eqs. (1.48) and (1.49)) and dots are from simulations. Note that at p_c there are large fluctuations. **b** Size of giant component, p_∞, in interdependent networks with both networks having clustering via Poisson degree distributions of Eq. (1.53) and average degree $\langle k\rangle = \mu_A + 2\nu_A = 4$, as a function of p. *Dashed lines* are number of interactions (NOI) before cascading failure stops obtained by simulation [74]. *Inset*: Green line is the critical threshold p_c in interdependent networks as function of clustering coefficient c. *Red* dashed line represents critical threshold of shuffled interdependent networks which originally has clustering coefficient c. The shuffled networks have zero clustering and degree-degree correlation, but has the same degree distribution as the original clustered networks. Symbols and *dashed lines* represent simulation, *solid curves* represent theoretical results. After [65]

result obtained in Ref. [44] for random interdependent ER networks. Figure 1.10, using numerical simulation, compares the size of the giant component after n stages of cascading failure with the theoretical prediction of Eq. (1.48). When $p = 0.7$ and $p = 0.64$, which are not near the critical threshold ($p_c = 0.6609$), the agreement with simulation is perfect. Below and near the critical threshold, the simulation initially agrees with the theoretical prediction but then deviates for large n due to the random fluctuations of structure in different realizations [44]. By solving Eq. (1.55), we have p_∞ as a function of p in Fig. 1.10 for a given average degree and several values of clustering coefficients. The figure shows that the interdependent networks with higher clustering become less robust than the networks with low clustering and the same average degree k, i.e., p_c is a monotonically increasing function of c (see inset of Fig. 1.10).

1.4 Application to Infrastructure

In interacting networks, the failure of nodes in one network generally leads to the failure of dependent nodes in other networks, which in turn may cause further damage to the first network, leading to cascading failures and catastrophic consequences. It is known, for example, that blackouts in various countries have been the result of cascading failures between interdependent systems such as communication and power grid systems [75] (Fig. 1.11). Furthermore, different kinds of critical infrastructures are also coupled together, e.g., systems of water and food supply, communications, fuel, financial transactions, and power generation and transmission (Fig. 1.11). Modern technology has produced infrastructures that are becoming increasingly interdependent, and understanding how robustness is affected by these interdependencies is one of the major challenges faced when designing resilient infrastructures [56, 58, 75, 76].

Blackouts are a demonstration of the important role played by the dependencies between networks. For example, the 28 September 2003 blackout in Italy resulted in a widespread failure of the railway network, healthcare systems, and financial services and, in addition, severely influenced communication networks. The partial failure of the communication system in turn further impaired the power grid management system, thus producing a negative feedback on the power grid. This example emphasizes how interdependence can significantly magnify the damage in an interacting network system [44, 45, 58, 75].

Thus understanding the coupling and interdependencies of networks will enable us to design and implement future infrastructures that are more efficient and robust.

1.5 Application to Finance and Economics

Financial and economic networks are neither static nor independent of one another. As global economic convergence progresses, countries increasingly depend on each other through such links as trade relations, foreign direct investments, and flow of funds in international capital markets. Economic systems such as real estate markets, bank borrowing and lending operations, and foreign exchange trading are interconnected and constantly affect each other. As economic entities and financial markets become increasingly interconnected, a shock in a financial network can provoke

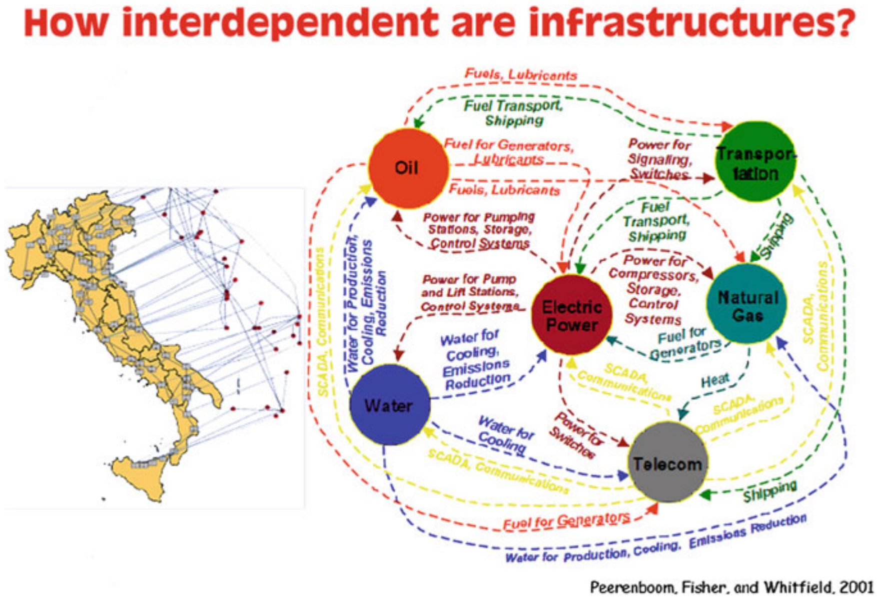

Fig. 1.11 *Left*: Power grid and Internet dependence in Italy. Analysis of this system can explain the cascade failure that led to the 2003 blackout. *Right*: Inter-dependence of fundamental infrastructures. A further example is a recent event in Cyprus (July 2011), where an explosion caused a failure of the electrical power lines, which in turn caused the countries water supply to shut down, due to the strong coupling between these two networks

significant cascading failures throughout the global economic system. Based on the success of complex networks in modeling interconnected systems, applying complex network theory to study economic systems has been given much attention [77–84].

The strong connectivity in financial and economic networks allows catastrophic cascading node failure to occur whenever the system experiences a shock, especially if the shocked nodes are hubs or are highly central in the network [7, 63, 76, 85, 86]. To thus minimize systemic risk, financial and economic networks should be designed to be robust to external shocks.

In the wake of the recent global financial crisis, increased attention has been given to the study of the dynamics of economic systems and to systemic risk in particular. The widespread impact of the current EU sovereign debt crisis and the 2008 world financial crisis show that, as economic systems become increasingly interconnected, local exogenous or endogenous shocks can provoke global cascading system failure that is difficult to reverse and that can cripple the system for a prolonged period of time. Thus policy makers are compelled to create and implement safety measures that prevent cascading system failures or that soften their systemic impact.

To study the systemic risk to financial institutions, we analyze a coupled (bipartite) bank-asset network in which a link between a bank and a bank asset exists when the bank has the asset on its balance sheet. Recently, Huang et al. [87] presented a model that focuses on real estate assets to examine banking network dependencies on real estate markets. The model captures the effect of the 2008 real estate market failure on the US banking network. Between 2000 and 2007, 27 banks failed in the US, but between 2008 and early 2013 the number rose to over 470. The model proposes a cascading failure algorithm to describe the risk propagation process during crises. This methodology was empirically tested with balance sheet data from US commercial banks for the year 2007, and model predictions are compared with the actual failed banks in the US after 2007 as reported by the Federal Deposit Insurance Corporation (FDIC). The model identifies a significant portion of the actual failed banks, and the results suggest that this methodology could be useful for systemic risk stress testing for financial systems. The model also indicates that commercial rather than residential real estate markets were the major culprits for the failure of over 350 US commercial banks during the period 2008–2011.

There are two main channels of risk contagion in the banking system, (i) direct interbank liability linkages between financial institutions and (ii) contagion via changes in bank asset values. The former, which has been given extensive empirical and theoretical study [88–92], focuses on the dynamics of loss propagation via the complex network of direct counterpart exposures following an initial default. The latter, based on bank financial statements and financial ratio analysis, has received scant attention. A financial shock that contributes to the bankruptcy of a bank in a complex network will cause the bank to sell its assets. If the financial market's ability to absorb these sales is less than perfect, the market prices of the assets that the bankrupted bank sells will decrease. Other banks that own similar assets could also fail because of loss in asset value and increased inability to meet liability obligations. This imposes further downward pressure on asset values and contributes to further asset devaluation in the market. Damage in the banking network thus continues to spread, and the result is a cascading of risk propagation throughout the system [93, 94].

Using this coupled bank-asset network model, we can test the influence of each particular asset or group of assets on the overall financial system. If the value of agricultural assets drop by 20 %, we can determine which banks are vulnerable to failure and offer policy suggestions, e.g., requiring mandatory reduction in exposure to agricultural loans or closely monitoring the exposed bank, to prevent such failure.

The model shows that sharp transitions can occur in the coupled bank-asset system and that the network can switch between two distinct regions, stable and unstable, which means that the banking system can either survive and be healthy or collapse. Because it is important that policy makers keep the world economic system in the stable region, we suggest that our model for systemic risk propagation might also be applicable to other complex financial systems, e.g., to model how sovereign debt value deterioration affects the global banking system or how the depreciation or appreciation of certain currencies impact the world economy.

1.5.1 Cascading Failures in the US Banking System

During the recent financial crisis, 371 US commercial banks failed between 1 January 2008 and 1 July 2011. The Failed Bank List from the Federal Deposit Insurance Corporation (FBL-FDIC) records the names of failed banks and the dates of their failure. We use this list as an experimental benchmark for our model. The dataset used as input to the model is the US Commercial Banks Balance Sheet Data (CBBSD) from Wharton Research Data Services, which contains the amount of assets in each category that the US commercial banks have on their balance sheets.

To build a sound bank-asset coupled system network and systemic risk cascading failure model, it is important to study the properties of the failed banks and compare them with the properties of the banks that survive. Thus the asset portfolios of commercial banks containing asset categories such as commercial loans or residential mortgages are carefully examined. The banks are modeled according to how they construct their asset portfolios (see the upper panel of Fig. 1.12). For each bank, the CBBSD contains 13 different non-overlapping asset categories, e.g., bank i owns amounts $B_{i,0}$, $B_{i,1}$, ..., $B_{i,12}$ of each asset, respectively. The total asset value B_i and total liability value L_i of a bank i are obtained from CBBSD dataset. The weight of each asset m in the overall asset portfolio of a bank i is then defined as $w_{i,m} \equiv B_{i,m}/B_i$. From the perspective of the asset categories, we define the *total market value* of an asset m as $A_m \equiv \sum_i B_{i,m}$. Thus the market share of bank i in asset m is $s_{i,m} \equiv B_{i,m}/A_m$.

Studying the properties of failed banks between 2008 and 2011 reveals that, for certain assets, asset weight distributions for all banks differ from the asset weight distributions for failed banks. Failed banks cluster in a region heavily weighted with construction and development loans and loans secured by nonfarm nonresidential properties while having fewer agricultural loans in their asset portfolios than the banks that survived. These results confirm the nature of the most recent financial crisis of 2008–2011 in which bank failures were largely caused by real estate-based loans, including loans for construction and land development and loans secured by nonfarm nonresidential properties [95]. In this kind of financial crisis, banks with greater agricultural loan assets are more financially robust [96]. Failed banks also tend to have lower equity-to-asset ratios, i.e., higher leverage ratios than the banks that survived during the financial crisis of 2008–2011 [97].

A financial crisis usually starts with the bursting of an economic or financial bubble. For example, with the bursting of the dot-com bubble, the technology-heavy NASDAQ Composite index lost 66 % of its value, plunging from 5048 in 10 March 2000 to 1720 in 2 April 2001. In our current model, the shock in the bank-asset coupled system originated with the real estate bubble burst. The two categories of real estate assets most relevant to the failure of commercial banks during the 2008–2011 financial crisis were construction and land development loans and loans secured by nonfarm and non-residential properties. Although it is widely believed that the financial crisis was caused by residential real estate assets, the coupled bank-asset network model does not find evidence that loans secured by 1–4 family

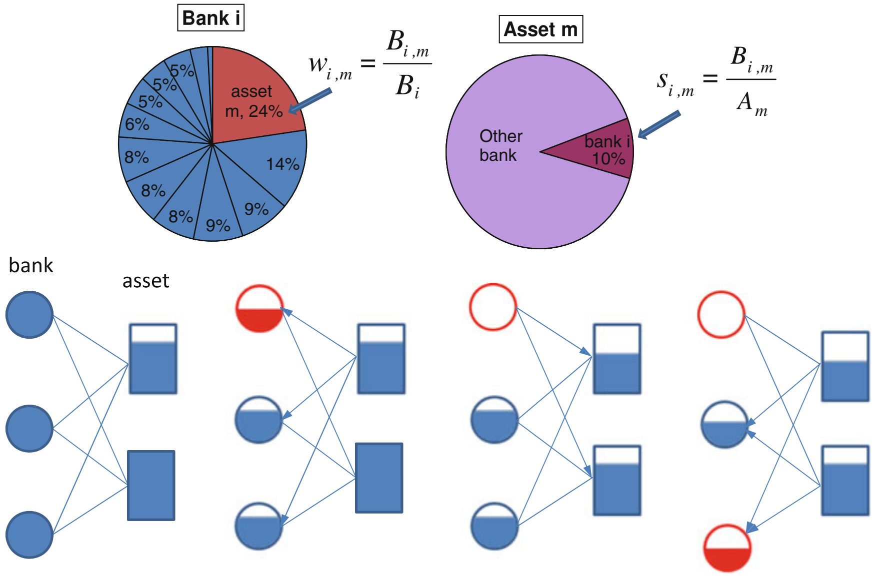

Fig. 1.12 Bank-asset coupled network model with banks as one node type and assets as the other node type. Link between a bank and an asset exists if the bank has the asset on its balance sheet. *Upper* panel: illustration of bank-node and asset-node. $B_{i,m}$ is the amount of asset m that bank i owns. Thus, a bank i with total asset value B_i has $w_{i,m}$ fraction of its total asset value in asset m. $s_{i,m}$ is the fraction of asset m that the bank holds out. *Lower* panel: illustration of the cascading failure process. The *rectangles* represent the assets and the *circles* represent the banks. From *left* to *right*, initially, an asset suffers loss in value which causes all the related banks' total assets to shrink. When a bank's remaining asset value is below certain threshold (e.g., the bank's total liability), the bank fails. Failure of the bank elicits disposal of bank assets which further affects the market value of the assets. This adversely affects other banks that hold this asset and the total value of their assets may drop *below* the threshold which may result in further bank failures. This cascading failure process propagates back and forth between banks and assets until no more banks fail. After [87]

residential properties were responsible for the commercial bank failures. This result is consistent with the conclusion of Ref. [95]: that the cause of commercial bank failure between 2008 and 2011 were commercial real estate-based loans rather than residential mortgages. For more details regarding the coupled bank-asset model see Ref. [87].

1.6 Summary and Outlook

In summary, this paper presents the recently-introduced mathematical framework of a Network of Networks (NON). In interacting networks, when a node in one network fails it usually causes dependent nodes in other networks to fail which, in turn, may cause further damage in the first network and result in a cascade of failures with catastrophic consequences. Our analytical framework enables us to follow the dynamic process of the cascading failures step-by-step and to derive steady state solutions. Interdependent networks appear in all aspects of life, nature, and technology. Examples include (i) transportation systems such as railway networks, airline networks, and other transportation systems [53, 98]; (ii) the human body as studied by physiology, including such examples of interdependent NON systems as the cardiovascular system, the respiratory system, the brain neuron system, and the nervous system [99]); (iii) protein function as studied by biology, treating protein interaction—the many proteins involved in numerous functions—as a system of interacting networks; (iv) the interdependent networks of banks, insurance companies, and business firms as studied by economics; (v) species interactions and the robustness of interaction networks to species loss as studied by ecology, in which it is is essential to understand the effects of species decline and extinction [100]; and (vi) the topology of statistical relationships between distinct climatologically variables across the world as studied by climatology [101].

Thus far only a few real-world interdependent systems have been thoroughly analyzed [53, 98]. We expect our work to provide insights leading further analysis of real data on interdependent networks. The benchmark models presented here can be used to study the structural, functional, and robustness properties of interdependent networks. Because in real-world NONs individual networks are not randomly connected and their interdependent nodes are not selected at random, it is crucial that we understand the many types of correlation that exist in real-world systems and that we further develop the theoretical tools to take them into account. Further studies of interdependent networks should focus on (i) an analysis of real data from many different interdependent systems and (ii) the development of mathematical tools for studying real-world interdependent systems. Many real networks are embedded in space, and the spatial constraints strongly affect their properties [20, 102, 103]. There is a need to understand how these spatial constraints influence the robustness properties of interdependent networks [98]. Other properties that influence the robustness of single networks, such as the dynamic nature of the configuration in which links or nodes appear and disappear and the directed nature of some links, as well as problems associated with degree-degree correlations and clustering, should be also addressed in future studies of coupled network systems. An additional critical issue is the improvement of the robustness of interdependent infrastructures. Our studies thus far shown that there are three methods of achieving this goal (i) by increasing the fraction of autonomous nodes [45], (ii) by designing dependency links such that they connect the nodes with similar degrees [44, 53], and (iii) by protecting the high-degree nodes against attack [33]. Achieving this goal will provide greater safety and stability in today's socio-techno world.

Networks dominate every aspect of present-day living. The world has become a global village that is steadily shrinking as the ways that human beings interact and connect multiply. Understanding these connections in terms of interdependent networks of networks will enable us to better design, organize, and maintain the future of our socio-techno-economic world.

Acknowledgments We wish to thank ONR (Grant N00014-09-1-0380, Grant N00014-12-1-0548), DTRA (Grant HDTRA-1-10-1- 0014, Grant HDTRA-1-09-1-0035), NSF (Grant CMMI 1125290), the European EPIWORK, MULTIPLEX, CONGAS (Grant FP7-ICT-2011-8-317672), FET Open Project FOC 255987 and FOC-INCO 297149, and LINC projects, DFG, the Next Generation Infrastructure (Bsik) and the Israel Science Foundation for financial support. SVB acknowledges the Dr. Bernard W. Gamson Computational Science Center at Yeshiva College.

References

1. D.J. Watts, S.H. Strogatz, Nature **393**(6684), 440 (1998)
2. A.L. Barabási, R. Albert, Science **286**(5439), 509 (1999)
3. M. Faloutsos, P. Faloutsos, C. Faloutsos, in *ACM SIGCOMM Computer Communication Review*, vol. 29 (ACM, 1999), vol. 29, pp. 251–262
4. R. Albert, H. Jeong, A.L. Barabási, Nature **406**(6794), 378 (2000)
5. R. Cohen, K. Erez, D. Ben-Avraham, S. Havlin, Physical Review Letters **85**(21), 4626 (2000)
6. D.S. Callaway, M.E. Newman, S.H. Strogatz, D.J. Watts, Physical Review Letters **85**(25), 5468 (2000)
7. R. Cohen, K. Erez, D. Ben-Avraham, S. Havlin, Physical Review Letters **86**(16), 3682 (2001)
8. R. Milo, S. Shen-Orr, S. Itzkovitz, N. Kashtan, D. Chklovskii, U. Alon, Science Signaling **298**(5594), 824 (2002)
9. D.J. Watts, Proceedings of the National Academy of Sciences **99**(9), 5766 (2002)
10. M.E.J. Newman, SIAM review **45**(2), 167 (2003)
11. A. Barrat, M. Barthelemy, R. Pastor-Satorras, A. Vespignani, Proceedings of the National Academy of Sciences of the United States of America **101**(11), 3747 (2004)
12. M.E.J. Newman, M. Girvan, Physical Review E **69**(2), 026113 (2004)
13. L.K. Gallos, R. Cohen, P. Argyrakis, A. Bunde, S. Havlin, Physical Review Letters **94**(18), 188701 (2005)
14. V. Latora, M. Marchiori, Physical Review E **71**(1), 015103 (2005)
15. C. Song, S. Havlin, H.A. Makse, Nature **433**(7024), 392 (2005)
16. S. Boccaletti, V. Latora, Y. Moreno, M. Chavez, D.U. Hwang, Physics Reports **424**(4), 175 (2006)
17. M.E.J. Newman, A.L. Barabasi, D.J. Watts, *The structure and dynamics of networks* (Princeton University Press, 2011)
18. B.J. West, P. Grigolini, *Complex webs: anticipating the improbable* (Cambridge University Press, 2010)
19. G. Bonanno, G. Caldarelli, F. Lillo, R.N. Mantegna, Physical Review E **68**(4), 046130 (2003)
20. D. Li, K. Kosmidis, A. Bunde, S. Havlin, Nature Physics **7**(6), 481 (2011)
21. D.Y. Kenett, M. Tumminello, A. Madi, G. Gur-Gershgoren, R. Mantegna, E. Ben-Jacob, PloS one **5**(12), e15032 (2010)
22. D.Y. Kenett, T. Preis, G. Gur-Gershgoren, E. Ben-Jacob, International Journal of Bifurcation and Chaos **22**(7), 1250181 (2012)
23. Y.N. Kenett, D.Y. Kenett, E. Ben-Jacob, M. Faust, PloS one **6**(8), e23912 (2011)
24. A. Madi, D. Kenett, S. Bransburg-Zabary, Y. Merbl, F. Quintana, S. Boccaletti, A. Tauber, I. Cohen, E. Ben-Jacob, Chaos**21**(1), 016109 (2011)
25. S. Bransburg-Zabary, D.Y. Kenett, G. Dar, A. Madi, Y. Merbl, F.J. Quintana, A.I. Tauber, I.R. Cohen, E. Ben-Jacob, Physical Biology **10**(2), 025003 (2013)
26. A. Majdandzic, B. Podobnik, S.V. Buldyrev, D.Y. Kenett, S. Havlin, H.E. Stanley, Spontaneous recovery in dynamical networks, Nature Physics, doi:10.1038/nphys2819 (2013)
27. E. López, S.V. Buldyrev, S. Havlin, H.E. Stanley, Physical Review Letters **94**(24), 248701 (2005)
28. M. Boguná, D. Krioukov, Physical Review Letters **102**(5), 058701 (2009)

29. V. Colizza, A. Barrat, M. Barthelemy, A. Vespignani, et al., Proc. Natl. Acad. Sci. USA 103 (2005)
30. Z. Wu, L.A. Braunstein, V. Colizza, R. Cohen, S. Havlin, H.E. Stanley, Physical Review E **74**(5), 056104 (2006)
31. R. Albert, A.L. Barabási, Reviews of modern physics **74**(1), 47 (2002)
32. A. Bunde, S. Havlin, *Fractals and disordered systems* (Springer, Berlin Heidelberg, 1991)
33. C.M. Schneider, A.A. Moreira, J.S. Andrade, S. Havlin, H.J. Herrmann, Proceedings of the National Academy of Sciences **108**(10), 3838 (2011)
34. Y. Chen, G. Paul, S. Havlin, F. Liljeros, H.E. Stanley, Physical Review Letters **101**(5), 058701 (2008)
35. R. Cohen, S. Havlin, D. Ben-Avraham, Physical Review Letters **91**(24), 247901 (2003)
36. L.A. Braunstein, S.V. Buldyrev, R. Cohen, S. Havlin, H.E. Stanley, Physical Review Letters **91**(16), 168701 (2003)
37. R. Pastor-Satorras, A. Vespignani, Physical review letters **86**(14), 3200 (2001)
38. D. Balcan, V. Colizza, B. Gonçalves, H. Hu, J.J. Ramasco, A. Vespignani, Proceedings of the National Academy of Sciences **106**(51), 21484 (2009)
39. G. Palla, I. Derényi, I. Farkas, T. Vicsek, Nature **435**(7043), 814 (2005)
40. G. Kossinets, D.J. Watts, Science **311**(5757), 88 (2006)
41. M.E.J. Newman, Proceedings of the National Academy of Sciences **98**(2), 404 (2001)
42. A.A. Moreira, J.S. Andrade Jr, H.J. Herrmann, J.O. Indekeu, Physical Review Letters **102**(1), 018701 (2009)
43. S. Havlin, D.Y. Kenett, E. Ben-Jacob, A. Bunde, R. Cohen, H. Hermann, J. Kantelhardt, J. Kertész, S. Kirkpatrick, J. Kurths, et al., European Physical Journal-Special Topics **214**(1), 273 (2012)
44. S. Buldyrev, R. Parshani, G. Paul, H. Stanley, S. Havlin, Nature **464**(7291), 1025 (2010)
45. R. Parshani, S.V. Buldyrev, S. Havlin, Physical Review Letters **105**(4), 048701 (2010)
46. J. Shao, S.V. Buldyrev, L.A. Braunstein, S. Havlin, H.E. Stanley, Physical Review E **8**0(3), 036105 (2009)
47. J. Gao, S.V. Buldyrev, H.E. Stanley, S. Havlin, Nature Physics **8**(1), 40 (2011)
48. M. Molloy, B. Reed, Combinatorics probability and computing **7**(3), 295 (1998)
49. P. Erdős, A. Rényi, Publ. Math. Debrecen **6**, 290 (1959)
50. P. Erdős, A. Rényi, Publ. Math. Inst. Hungar. Acad. Sci **5**, 17 (1960)
51. B. Bollobás, *Graph theory*, vol. 62 (North Holland, 1982)
52. S.V. Buldyrev, N.W. Shere, G.A. Cwilich, Physical Review E **83**(1), 016112 (2011)
53. R. Parshani, C. Rozenblat, D. Ietri, C. Ducruet, S. Havlin, EPL (Europhysics Letters) 92(6), 68002 (2010)
54. D. Gaogao, J. Gao, R. Du, L. Tian, H.E. Stanley, S. Havlin, Robustness of network of networks under targeted attack, Physical Review **87**(5), 052804 (2013)
55. D. Cellai, E. López, J. Zhou, J.P. Gleeson, G. Bianconi, Percolation in multiplex networks with overlap, Physical Review **88**(5), 052811 (2013)
56. J. Shao, S.V. Buldyrev, S. Havlin, H.E. Stanley, Physical Review E **83**(3), 036116 (2011)
57. C.M. Schneider, N.A. Araujo, S. Havlin, H.J. Herrmann, arXiv:1106.3234 [cond-mat.stat-mech] (2011)
58. S.M. Rinaldi, J.P. Peerenboom, T.K. Kelly, Control Systems, IEEE **21**(6), 11 (2001)
59. J. Gao, S.V. Buldyrev, S. Havlin, H.E. Stanley, Physical Review Letters **107**(19), 195701 (2011)
60. Gao et al, Percolation of a general network of networks, PRE (in press, 2014)
61. J. Gao, S. Buldyrev, S. Havlin, H. Stanley, Physical Review E **85**(6), 066134 (2012)
62. P. Holme, B.J. Kim, C.N. Yoon, S.K. Han, Physical Review E **65**(5), 056109 (2002)
63. X. Huang, J. Gao, S.V. Buldyrev, S. Havlin, H.E. Stanley, Physical Review E **83**(6), 065101 (2011)
64. T. Tanizawa, S. Havlin, H.E. Stanley, Physical Review E **85**(4), 046109 (2012)
65. X. Huang, S. Shao, H. Wang, S.V. Buldyrev, H.E. Stanley, S. Havlin, EPL (Europhysics Letters) **101**(1), 18002 (2013)

66. D. Zhou, H.E. Stanley, G. D'Agostino, A. Scala, Phys. Rev. E **86**, 066103 (2012)
67. M.A. Serrano, M. Boguna, Physical Review E **74**(5), 056114 (2006)
68. M.E.J. Newman, Physical Review Letters **103**(5), 058701 (2009)
69. J.C. Miller, Physical Review E **80**(2), 020901 (2009)
70. J.P. Gleeson, S. Melnik, Physical Review E **80**(4), 046121 (2009)
71. J.P. Gleeson, S. Melnik, A. Hackett, Physical Review E **81**(6), 066114 (2010)
72. C. Molina, L. Stone, Journal of Theoretical Biology (2012)
73. B. Karrer, M.E.J. Newman, Physical Review E **82**(6), 066118 (2010)
74. R. Parshani, S.V. Buldyrev, S. Havlin, Proceedings of the National Academy of Sciences **108**(3), 1007 (2011)
75. V. Rosato, L. Issacharoff, F. Tiriticco, S. Meloni, S. Porcellinis, R. Setola, International Journal of Critical Infrastructures **4**(1), 63 (2008)
76. A. Vespignani, Nature **464**(7291), 984 (2010)
77. R.M. May, S.A. Levin, G. Sugihara, Nature **451**(7181), 893 (2008)
78. A. Garas, P. Argyrakis, C. Rozenblat, M. Tomassini, S. Havlin, New journal of Physics **12**(11), 113043 (2010)
79. N. Johnson, T. Lux, Nature **469**(7330), 302 (2011)
80. A.G. Haldane, R.M. May, Nature **469**(7330), 351 (2011)
81. F. Schweitzer, G. Fagiolo, D. Sornette, F. Vega-Redondo, A. Vespignani, D.R. White, science **325**(5939), 422 (2009)
82. S. Battiston, M. Puliga, R. Kaushik, P. Tasca, G. Caldarelli, Scientific Reports **2** (2012)
83. D.Y. Kenett, M. Raddant, T. Lux, E. Ben-Jacob, PloS one **7**(2), e31144 (2012)
84. D.Y. Kenett, M. Raddant, L. Zatlavi, T. Lux, E. Ben-Jacob, International Journal of Modern Physics Conference Series **16**(1), 13 (2012)
85. A.E. Motter, Y.C. Lai, Physical Review E **66**(6), 065102 (2002)
86. A.G. Smart, L.A. Amaral, J.M. Ottino, Proceedings of the National Academy of Sciences **105**(36), 13223 (2008)
87. X. Huang, I. Vodenska, S. Havlin, H.E. Stanley, Scientific reports **3** (2013)
88. S. Wells, Financial Stability Review **13**, 175 (2002)
89. C.H. Furfine, Journal of Money, Credit and Banking pp. 111–128 (2003)
90. C. Upper, A. Worms, European Economic Review **48**(4), 827 (2004)
91. H. Elsinger, A. Lehar, M. Summer, Management science **52**(9), 1301 (2006)
92. E. Nier, J. Yang, T. Yorulmazer, A. Alentorn, Journal of Economic Dynamics and Control **31**(6), 2033 (2007)
93. R. Cifuentes, G. Ferrucci, H.S. Shin, Journal of the European Economic Association **3**(2–3), 556 (2005)
94. I. Tsatskis, Available at SSRN 2062174 (2012)
95. R.A. Cole, L.J. White, Journal of Financial Services Research **42**(1–2), 5 (2012)
96. G.S. Corner, Central Banker (Fall) (2011)
97. Y. Gopalan, Central Banker (Spring) (2010)
98. C.G. Gu, S.R. Zou, X.L. Xu, Y.Q. Qu, Y.M. Jiang, H.K. Liu, T. Zhou, et al., Physical Review E **84**(2), 026101 (2011)
99. A. Bashan, R.P. Bartsch, J.W. Kantelhardt, S. Havlin, P.C. Ivanov, Nature communications **3**, 702 (2012)
100. M.J. Pocock, D.M. Evans, J. Memmott, Science **335**(6071), 973 (2012)
101. J.F. Donges, H.C. Schultz, N. Marwan, Y. Zou, J. Kurths, The European Physical Journal B **84**(4), 635 (2011)
102. M. Barthélemy, Physics Reports **499**(1), 1 (2011)
103. W. Li, A. Bashan, S.V. Buldyrev, H.E. Stanley, S. Havlin, Physical Review Letters **108**(22), 228702 (2012)